Nature and Science of Sleep

Elevate Series

Open Access Full Text Article

ORIGINAL RESEARCH

The Role of Ferroptosis in Adenoid Hypertrophy in Children with Obstructive Sleep Apnea Syndrome

Zilu Shen[1,*], Jingning Huang[2,*], Yunqiu Chu[2], Xiaoman Zhang[2], Huajun Xu[2], Hongming Xu[1], Jian Guan[2], Meizhen Gu[1]

[1]Department of Otorhinolaryngology Head and Neck Surgery, Shanghai Children's Hospital, School of Medicine, Shanghai Jiao Tong University, Shanghai, 200062, People's Republic of China; [2]Department of Otolaryngology Head and Neck Surgery, Shanghai Sixth People's Hospital, Shanghai Jiao Tong University, Shanghai, 200233, People's Republic of China

*These authors contributed equally to this work

Correspondence: Hongming Xu; Meizhen Gu, Department of Otorhinolaryngology Head and Neck Surgery, Shanghai Children's Hospital, School of Medicine, Shanghai Jiao Tong University, Shanghai, 200062, People's Republic of China, Email xuhongming@188.com; gumz@shchildren.com.cn

Purpose: Obstructive sleep apnea (OSA) is a common sleep disorder in children, with adenoid hypertrophy was recognized as the main cause. While ferroptosis has been linked to adult OSA, its role in children with adenoid hypertrophy remains unclear. Here, we aimed to explore the potential role of ferroptosis in pediatric OSA-associated adenoid hypertrophy.

Methods: We conducted RNA sequencing on adenoid tissues from children with OSA stratified by severity (mild-to-moderate, n=9; severe, n=9). Hub genes were identified by integrating differentially expressed genes (DEGs) with ferroptosis-related genes and constructing a protein–protein interaction (PPI) network. We further validated these findings in an independent cohort and primary cells.

Results: KEGG enrichment analysis revealed significant alterations in ferroptosis-related pathways, including p53 signaling pathway and Glutathione metabolism ($p < 0.05$). We identified 108 ferroptosis-related DEGs (fold change: 0.45–6.42, adjusted $p < 0.05$) and subsequently pinpointed 8 hub genes through PPI network construction and Cytoscape analysis (fold change:0.61–1.81, adjusted $p < 0.05$). In clinical sample validation, mild-to-moderate tissues exhibited significant activation of ferroptosis. With the exception of *PLA2G7*, the expression trends of the other 7 hub DEGs were consistent with the findings from bioinformatics analysis. Moreover, ferroptosis inducers significantly suppressed the proliferation of adenoid primary cells in vitro (inhibition rate ≈70%, $p < 0.0001$).

Conclusion: This study helps us better understand how ferroptosis contributes to adenoid hypertrophy in children with OSA and also suggests that ferroptosis activation may attenuate disease advancement. Furthermore, the 7 hub genes are proposed as potential biomarkers and drug-binding targets.

Keywords: ferroptosis, adenoid hypertrophy, bioinformatic analysis, obstructive sleep apnea

Introduction

Pediatric obstructive sleep apnea (OSA) is a common sleep apnea disorder, which is caused by recurrent partial or complete upper airway obstruction during sleep.[1] Adenoid hypertrophy is recognized as the primary cause of pediatric OSA.[2] Under repeated inflammatory stimulation, adenoids are prone to pathological hyperplasia, leading to symptoms such as nasal obstruction, mouth breathing, and snoring.[3] If untreated, adenoid hypertrophy can result in adenoid facies, behavioral problems, and impaired growth and development, posing long-term risks to children's physical and mental health.[4] Despite its notable clinical impact, the underlying mechanisms of pediatric adenoid hypertrophy remain poorly understood. Previous studies have suggested potential links to immune responses, hormonal factors, and genetic predisposition.[3] For example, the upregulation of interleukin (IL)-32 in adenoid tissue exacerbates hypertrophy by activating NLRP3-mediated pyroptosis and promoting inflammation.[5] Additionally, children with adenoid hypertrophy often exhibit elevated levels of oxidative stress.[6] However, these studies have not fully clarified the specific immune signaling pathways, the contribution of oxidative stress, or the tissue remodeling processes involved in adenoid hypertrophy. Therefore, it is essential to investigate the pathogenesis of adenoid hypertrophy in children in depth, so as to develop novel therapeutic strategies.

Received: 10 September 2025
Accepted: 5 December 2025
Published: 18 December 2025

Ferroptosis is a form of cell death caused by iron buildup and oxidative stress, which is characterized by Glutathione (GSH) depletion, Fe^{2+} overload, and reactive oxygen species (ROS) accumulation.[7] Growing evidence indicates that ferroptosis plays a key role in hypoxia-related diseases, including hypoxic brain injury and myocardial infarction.[8,9] Recent studies have demonstrated ferroptosis was closely related with OSA.[10,11] OSA characteristic chronic intermittent hypoxic environment could lead to persistent accumulation of ROS.[12] Moreover, OSA patients exhibit disturbances in iron metabolism, with serum iron overload and ferritin levels positively correlated with disease severity.[13] In OSA-targeted organs such as the liver and brain, dysregulated expression of ferroptosis-related biomarkers has been observed, supporting a potential role in OSA pathophysiology.[14,15] We hypothesize that ferroptosis could also contributes to adenoid hypertrophy. Although the role of ferroptosis in adenoid hypertrophy remains unclear, elucidating its involvement may not only clarify its underlying pathophysiology but also support the identification of novel biomarkers and therapeutic targets that could improve clinical management in pediatric OSA. Therefore, this study aimed to investigate whether ferroptosis contributes to adenoid hypertrophy in children with OSA and to identify key genes involved in this process.

In this study, we first conducted transcriptome sequencing of adenoids and screened for hub genes by intersecting DEGs with genes in FerrDb database. Then, we validated the results on adenoid tissue and explored the role of ferroptosis in primary adenoid cells. Our study offers new insights into the underlying mechanisms and highlights potential therapeutic targets for adenoid hypertrophy.

Materials and Methods

Patients

This study enrolled children aged 3–12 years who underwent adenoidectomy at Shanghai Children's Hospital between May 2024 to September 2024. All participants were diagnosed with OSA by standard polysomnography, with an apnea-hypopnea index (AHI) ≥1, and were confirmed to have adenoid hypertrophy through imaging examinations by lateral cephalometric radiographs or fiberoptic endoscopy. Adenoid hypertrophy was graded based on choanal obstruction: Grade 1= 0–25% obstruction; Grade 2 = 25–50% obstruction; Grade 3 = 50–75% obstruction; Grade 4 = 75% or more obstruction. Based on this grading system, patients were categorized into two groups: mild-to-moderate hypertrophy group (Grade 1–3) and severe hypertrophy group (Grade 4). Exclusion criteria included recent infections, asthma, genetic disorders or other chronic diseases, and antibiotic use within two months prior to their visit. Body mass index (BMI) was calculated as weight/height^2 (kg/m^2). We ensured that the body mass index (BMI) distribution was balanced between the two groups during the enrollment phase to prevent it from being a major confounding variable.

A total of 18 pediatric patients were included in this study for RNA-seq analysis. This sample size was deemed sufficient to detect statistically significant differences, based on precedents established in prior research.[16]

Tissue Collection

Due to ethical constraints, adenoid tissue from healthy children was unavailable. Participants were graded preoperatively and categorized into mild-to-moderate and severe groups. Adenoid tissue was obtained by plasma radiofrequency-assisted ablation under general anesthesia. The excised tissues were immediately placed in liquid nitrogen and stored at −80°C. All intraoperative sampling procedures were performed by an experienced physician.

RNA Sequencing Analysis

Total RNA was isolated from adenoid tissue using TRIzol reagent (15596026CN, Invitrogen, CA, USA) according to the manufacturer's instructions and the concentration and quality were evaluated. Extracted mRNA was enriched and fragmented via high-temperature incubation. After reverse transcription to cDNA, the PCR library was then amplified and finally assayed using Illumina Novaseq X Plus (Illumina, CA, USA).

Differential Expression Analysis and Functional Enrichment Analysis

Using DESeq2 software to analyze DEGs between two groups, genes with adjusted p-value below 0.05 and absolute fold change value greater than to 1.4 were considered significant. Volcano plots were generated to visualize DEGs. Gene

ontology (GO) enrichment analysis was performed to assess molecular function (MF), cellular component (CC), and biological process (BP), with gene counts and adjusted p-values calculated for each term. Kyoto Encyclopedia of Genes and Genomes (KEGG) pathway analysis identified significantly enriched metabolic and signaling pathways associated with DEGs, using an adjusted p-value <0.05 as the threshold.

Screening Ferroptosis-Related DEGs

Ferroptosis-related DEGs were identified by intersecting DEGs with genes from the FerrDb database and visualized using Venn diagrams. These genes were subjected to GO and KEGG enrichment analyses. The identified genes were uploaded to the STRING online platform (https://string-db.org/) to construct a protein-protein interaction (PPI) network with a minimum interaction score of 0.4, hiding disconnected nodes. Subsequently, Cytoscape software (version 3.10.3) is employed to visualize and analyze the network, followed by in-depth analysis using Molecular Complex Detection (MCODE) and CytoHubba plugins. The parameters were set as degree cutoff = 2, node score cutoff = 0.2, k hub = 2 and max depth = 100.

Adenoid Primary Cell Culture

Surgically resected adenoids were used to isolate cells and establish mixed cell cultures. The adenoid tissue was cut into small fragments, and syringe plunger was used to grind the tissue and pass the contents through a 70um cell strainer (FSTR072, Beyotime, Shanghai, China) to obtain a cell suspension. Mononuclear cells were isolated using Ficoll-Paque (17544202, Cytiva, MA, USA) density gradient centrifugation at a density of 1.077 g/mL and cultured in RPMI1640 (E600028, Sangon Biotech, Shanghai, China) supplemented with 10% FBS (10099–141C, Gibco, NY, USA), 100 units/mL penicillin, and 100 ug/mL streptomycin (C100C5, NCM Biotech, Suzhou, China) at 37°C with 5% CO_2 for 24 h.

To simulate adenoid hypertrophy in vitro, 25 mg/mL lipopolysaccharide (LPS, L2630, Sigma-Aldrich, MO, USA) and 10 mg/mL concanavalin A (conA, C5275, Sigma-Aldrich, MO, USA) were added to the culture medium.[17] After 24 hours, cells were pretreated with 0 or 5μM Ferrostatin-1 (Fer-1, HY-100579, MedChemExpress, NJ, USA) for 2 hours, followed by 3μM RSL3 (Cat.HY-100218A, MedChemExpress, NJ, USA) for 24 hours, and proceed with subsequent experiments.

Cell Counting Kit-8 Assay

Cell viability was measured using the Cell Counting Kit-8 (CCK-8, HY-K0301, MedChemExpress, NJ, USA). Cells were seeded in 96-well plates at 1×10^6 cells/well. After treatments, 10 μL CCK-8 solution was added to each well according to the manufacturer's instructions and incubated at 37°C for 3 hours followed by measurement of absorbance at 450 nm.

RNA Isolation and Quantitative Real-Time PCR

Total RNA was extracted using Universal RNA Purification Kit (EZB-RN4, EZBioscience, MN, USA) and reverse transcription was performed with the Color Reverse Transcription Kit (A0010CGQ, EZBioscience, MN, USA). qPCR was then carried out using the Color SYBR Green qPCR Master Mix (A0012-R2, EZBioscience, MN, USA), with GAPDH as the internal control. Primer sequences are listed in the Table S1. The relative gene expression was calculated using the 2– ΔΔCT method.

Transmission Electron Microscopy (TEM)

Fresh adenoid tissues were sectioned into 1 mm^3 pieces on ice. The tissue fragments were fixed with 2.5% glutaraldehyde, followed by post-fixation with 1% aqueous osmium tetroxide. After graded ethanol and acetone dehydration, samples were embedded in epoxy resin. Ultrathin sections were double-stained with uranyl acetate and lead citrate. Ultrastructural images were captured using transmission electron microscopy (JEM-1230, JEOL, Japan).

ROS Measurements

To evaluate the production of ROS, DHE staining for tissues (S0063, Beyotime, Shanghai, China) and DCFH-DA staining for cells (S0033S, Beyotime, Shanghai, China). In brief, fresh-frozen tissue sections or cells were incubated at room temperature or 37°C for 30 minutes in the dark, followed by analysis using fluorescence microscopy.

GSH Level and MDA Level Assay

GSH content in adenoid tissues and cells were detected using Reduced glutathione assay kit (A006-2-1, Nanjing Jiancheng Bioengineering Institute, Nanjing, China). The level of MDA was determined using Lipid Peroxidation MDA Assay Kit (S0131S, Beyotime, Shanghai, China). Protein concentrations were quantified using BCA protein assay kit (ZJ102, EpiZyme, Shanghai, China) to normalize MDA levels.

Fe^{2+} Assay

Measured the ferrous ion levels in tissues using Ferrous Ion Content Assay Kit (BC5415, Solarbio, Beijing, China). Adenoid tissues were homogenized in buffer on ice, centrifuged at 10,000×g for 10 minutes at 4°C and 200 μL supernatant mixed with 100 μL of working solution. After incubation at 37°C for 10 minutes, absorbance was measured at 593 nm. Generate a standard curve simultaneously according to the manufacturer's instructions.

Western Blot Assay

Tissues or cultured cells were lysed in RIPA Lysis Buffer (P0013B, Beyotime, Shanghai, China) and were quantified using BCA protein assay kits. Proteins were separated by SDS-PAGE, transferred to nitrocellulose membranes, and blocked with 5% non-fat milk powder in TBST for 1 hour at room temperature. Then incubated with primary antibody overnight at 4°C: GPX4 (1:1500, A11243, Abclonal, Wuhan, China), β-actin (1:6000, 66,009-1-Ig, Proteintech, IL, USA), followed by 1 hour incubation with secondary antibodies and detection using ECL (SQ202, EpiZyme, Shanghai, China). Band intensities were quantified with ImageJ.

Statistical Analysis

Data were analyzed using GraphPad Prism 10.2. Comparisons between two groups were performed using the *t*-test, Mann–Whitney *U*-test, or chi-square test, while differences among three or more groups were analyzed using one-way ANOVA. Data were presented as mean±standard deviation (SD) when normally distributed, or as median with interquartile range (IQR) otherwise. Categorical variables were presented as counts (percentages). $P < 0.05$ was considered statistically significant.

Results

DEGs and Functional Enrichment Analysis in Adenoid from Severe and Mild-to-Moderate Hypertrophy

In this study, 18 pediatric OSA patients indicated for adenotonsillectomy (mild-to-moderate vs severe, n=9 for each group) were enrolled for RNA-seq, there were no significant differences between the two groups except for the degree of adenoid hypertrophy (Table 1).

We performed Principal Component Analysis to assess the overall variation in gene expression profiles (Figure 1A). Compared with mild-to-moderate group, there were 1615 genes up-regulated and 540 genes down-regulated in the severe group (Figure 1B). Although KEGG and GO analyses did not directly enrich the ferroptosis pathway, KEGG results showed that DEGs were involved in glutathione metabolism and P53 signaling pathway (Figure 1C), both closely associated with ferroptosis.[18,19] The expression patterns of these DEGs in these two pathways were shown in Figure 1D. Therefore, significant differences in gene expression were observed between the two groups, primarily enriched in glutathione metabolism and P53 signaling pathway.

Table 1 Baseline Demographic and Polysomnography Characteristics of Participants

	Mild-to-Moderate (n=9)	Severe (n=9)	Total (n=18)	P value
Mean Age (years)	5.6±2.33	5.7±1.81	5.6±2.03	0.902[a]
Gender (male, %)	7 (77.8%)	5 (55.6%)	12 (66.7%)	0.735[b]
BMI (kg/m^2)	15.18 (14.55–21.75)	15.42 (13.26–16.94)	15.30 (14.08–17.95)	0.399[c]
Adenoid size grade, n (%)				
Grade 2	4 (44.4%)	0 (0%)	4(22.2%)	
Grade 3	5 (55.6%)	0 (0%)	5(27.8%)	
Grade 4	0 (0%)	9 (100%)	9(50%)	<0.0001[b]
AHI	5.00 (2.69–15.56)	5.60 (3.17–14.69)	5.53 (3.16–14.80)	0.605[c]
Minimum SaO_2	91.11±4.17	89.11±5.65	90.11±4.92	0.405[a]
ODI	10.20±7.52	15.35±9.48	12.78±8.71	0.221[a]

Notes: Continuous data with a normal distribution are presented as mean ± SD, skewed data are presented as median (IQR). Categorical data are presented as number (percentage, %). [a]t-test. [b]chi-square test. [c]mann–Whitney *U*-test.
Abbreviations: BMI, body mass index; AHI, apnea-hypopnea index; SaO_2, oxygen saturation; ODI, oxygen desaturation index.

Ferroptosis-Related DEGs in Adenoid Hypertrophy

To further investigate the role of ferroptosis in adenoid hypertrophy, we obtained a dataset of 1290 ferroptosis-related genes from FerrDb database. Intersection of this gene set with the DEGs from our transcriptome and identified 108 ferroptosis-related DEGs (Figures 2A and S1), which were further classified as ferroptosis drivers, inhibitors, markers, and unclassified (Table S2). Subsequently, we performed GO enrichment analyses of these ferroptosis-related DEGs (Figure 2B). To determine the interactions among ferroptosis-related DEGs, we used the STRING online platform to analyze the PPI of these DEGs. The PPI network graph contains a total of 49 nodes and 47 edges (Figure 2C). To identify ferroptosis-related hub DEGs, we used the MCODE plugin for functional module analysis. A total of three functional modules comprising 11 genes were identified by MCODE analysis (Figure 2D). We further employed the CytoHubba plugin to analyze PPI network again based on the MCC algorithm, and obtained the top 10 hub genes in terms of degree value (Figure 2E). Combining these two algorithms, we obtained 8 hub genes, including *HSPA1B, HSPA13, HSPA14, HSPA1A, PLTP, PLA2G7, HDLBP, LDLR* (Table S3). Subsequently, the transcription levels of these hub genes were validated by qRT-PCR in a new set of independent adenoid samples. Compared to the mild-to-moderate group, transcript levels of *HSPA1B, HSPA1A, PLTP, HDLBP, LDLR* were significantly increased ($P < 0.05$), while *HSPA13, HSPA14* were significantly lower in the severe group ($P < 0.05$). However, there was no significant difference in expression of *PLA2G7* between two groups (Figure 2F and Table S4). Collectively, ferroptosis was closely associated with the development of adenoid hypertrophy.

Our analysis converged on a network of 8 hub genes, which functionally clustered into two major modules: a stress-responsive HSP70 cohort (*HSPA1A, HSPA1B, HSPA13, HSPA14*) and a lipid metabolism cluster (*PLTP, PLA2G7, HDLBP, LDLR*). The coordinated presence of these modules strongly suggests an integrated adaptive pathway that enhances cellular resistance to ferroptosis, thereby contributing to the pathogenesis of adenoid hypertrophy.

Ferroptosis Is Reduced in Severe Adenoid Hypertrophy

Based on the above bioinformatics analysis results, we collected a cohort of adenoid tissues to verify whether the identified hub genes are associated with the ferroptosis- related phenotypes. The results showed that GSH levels significantly higher in the severe group compared to the mild-to-moderate group (Figure 3A). As ferroptosis is characterized by intracellular iron overload and lipid peroxidation, we measured the levels of Fe^{2+} and MDA in adenoid tissues, which were both markedly lower in the severe group (Figure 3B and C). Excess Fe^{2+} can generate ROS through the Fenton reaction, thereby inducing ferroptosis.[7] Therefore, we performed ROS detection on fresh-frozen adenoid tissue sections using DHE. The results demonstrated that ROS levels in the mild-to-moderate hypertrophy group were statistically significantly higher than those in the severe hypertrophy group (Figure 3D). Concurrently, TEM showed that mitochondria from mild-to-moderate hypertrophy group exhibited characteristic alterations of ferroptosis, including

https://doi.org/10.2147/NSS.S566579

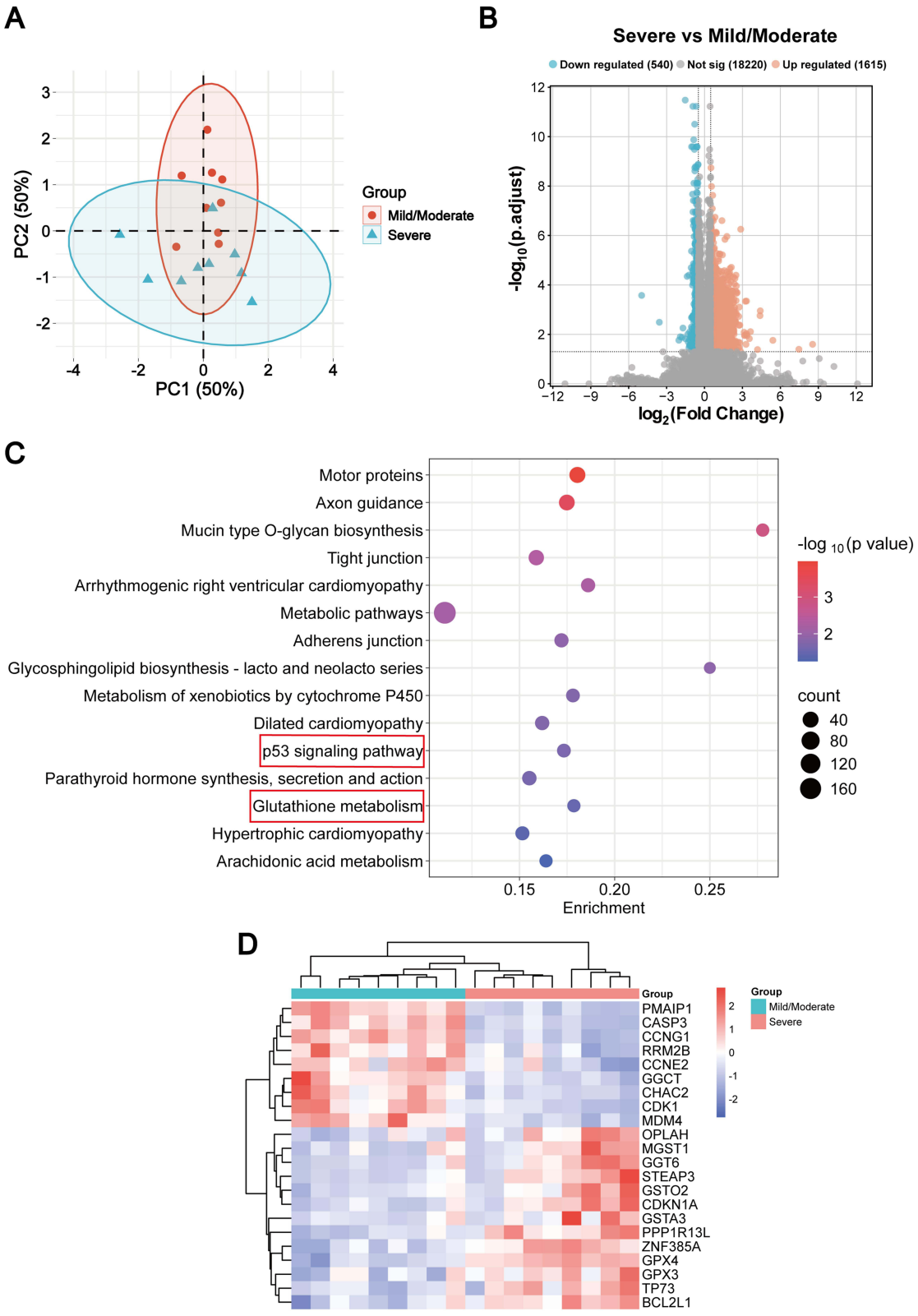

Figure 1 DEGs and functional enrichment analysis between mild-to-moderate and severe groups. (**A**) Principal component analysis between the two groups. (**B**) Volcano plot of DEGs. Red dots represent upregulated genes, blue dots represent downregulated genes, and gray dots represent unchanged genes. (**C**) KEGG pathway enrichment analysis was performed based on differentially expressed genes, showing the top 15 significantly enriched pathways. (**D**) Clustered heatmap displaying differentially expressed genes enriched in glutathione metabolism and p53 signaling pathways.

https://doi.org/10.2147/NSS.S566579

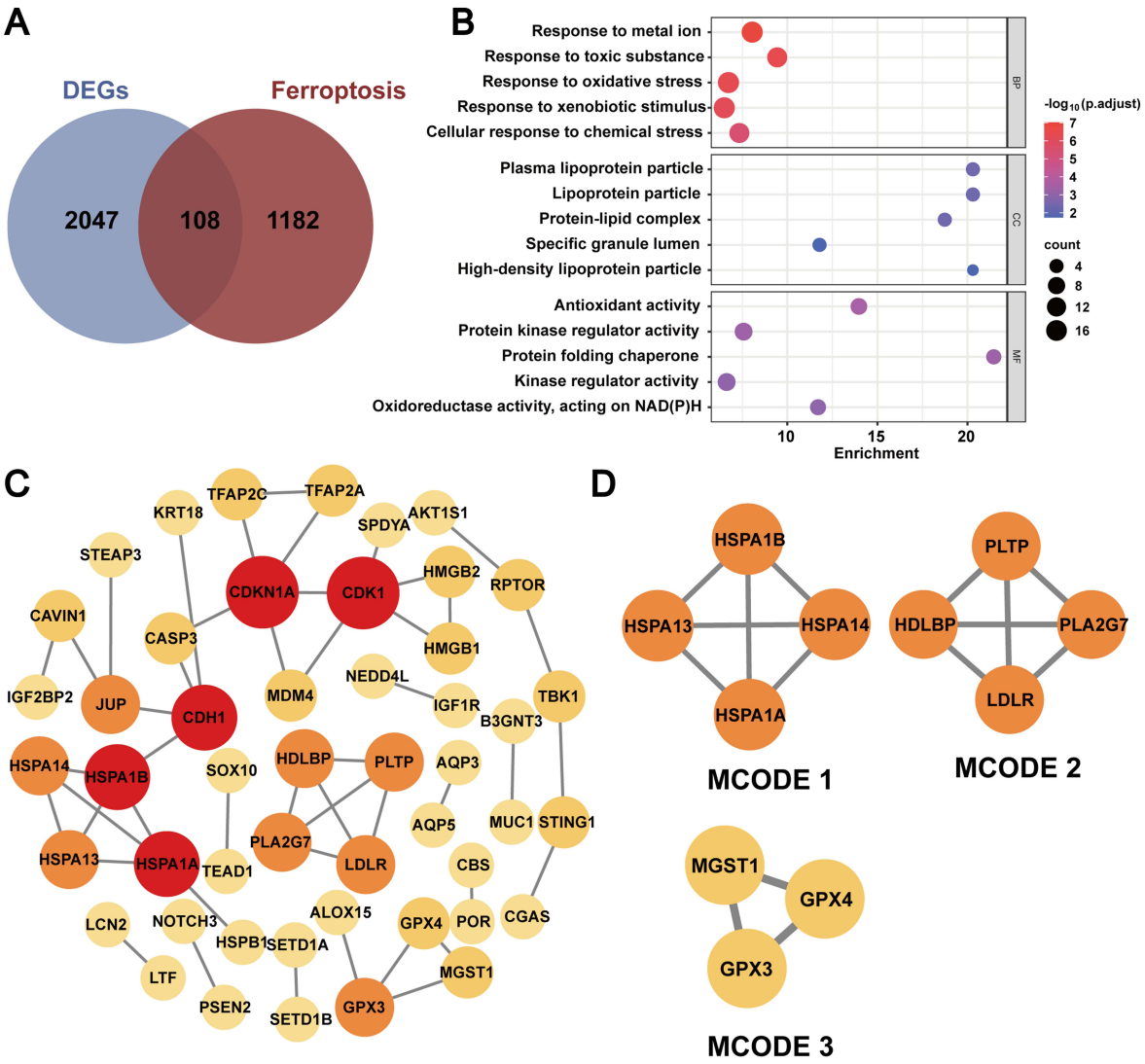

Figure 2 Identification and analysis of ferroptosis-related DEGs in adenoid hypertrophy. (**A**) Venn diagram shows the intersection between FerrDb genes and DEGs. (**B**) GO enrichment analysis results of ferroptosis-related DEGs. (**C**) PPI network of ferroptosis-related DEGs. (**D**) Three functional modules identified by MCODE analysis. (**E**) Top 10 hub genes identified by CytoHubba. (**F**) The mRNA expression of ferroptosis-related hub genes in adenoid tissues from mild-to-moderate and severe groups, n=5, data are presented as fold change relative to the mild to moderate group (set as 1). Statistical significance was determined by *t*-test. ns, not significant. Compared with the mild-to-moderate group, *P < 0.05, ***P < 0.001 and ****P< 0.0001.

https://doi.org/10.2147/NSS.S566579

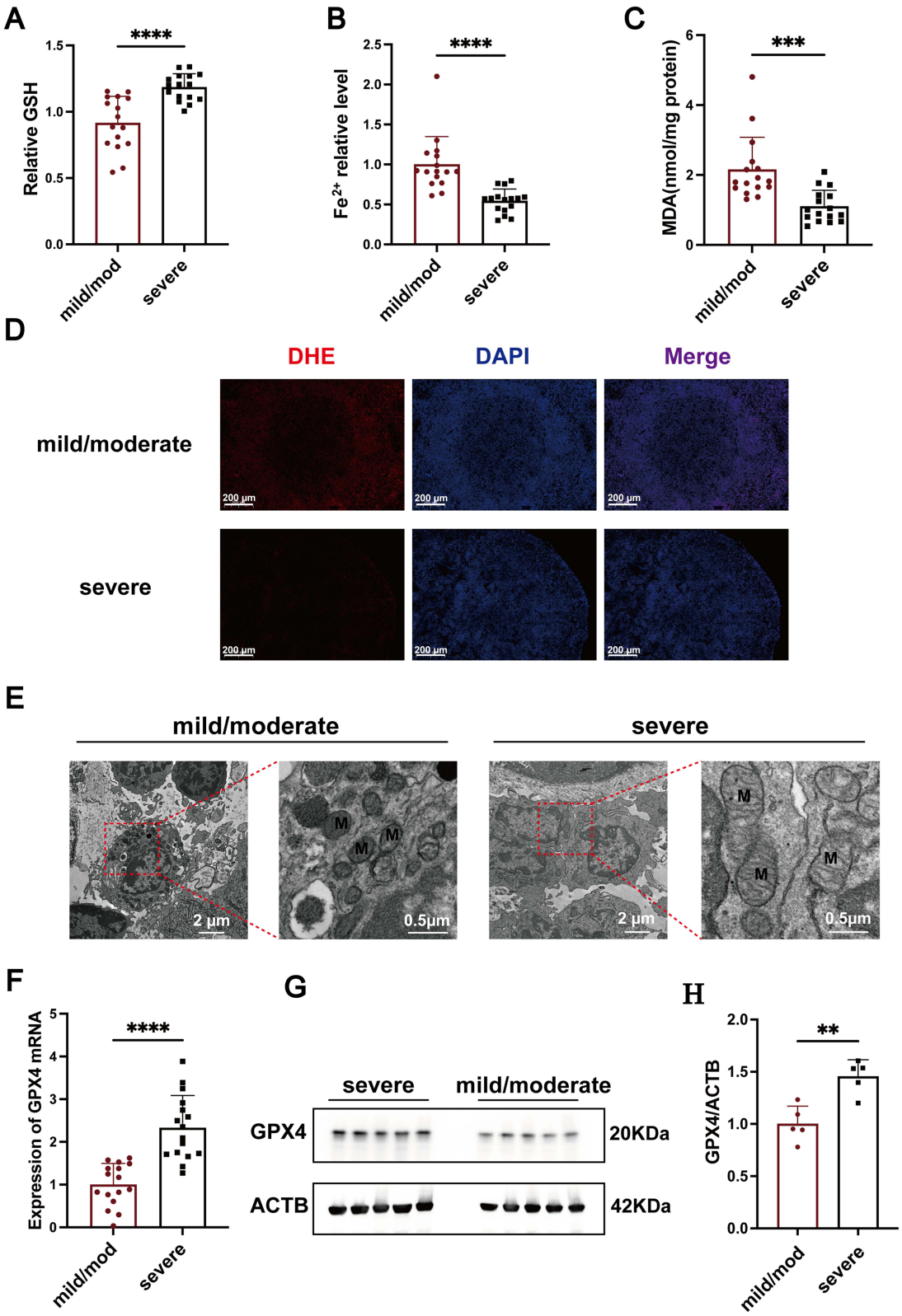

Figure 3 Ferroptosis is suppressed in tissues with severe adenoid hypertrophy. (**A**) GSH levels in adenoid tissue, n=16 per group. (**B**) Ferrous ion content in adenoid tissue, n=16 per group. (**C**) MDA level in adenoid tissue, n=16 per group. (**D**) Representative DHE staining images of adenoid tissue. (**E**) Representative TEM images of adenoid tissue, M, mitochondria. (**F**) Relative expression of *GPX4* mRNA in adenoid tissue, n=16 per group. (**G** and **H**) Representative Western blot bands and average protein levels of GPX4 in adenoids from the two groups, n=5 per group. Statistical significance was determined by *t*-test. Compared with the mild-to-moderate group, **P < 0.01, ***P < 0.001 and ****P< 0.0001.

irregular morphology and increased membrane density (Figure 3E). In addition, Western blotting and qRT-PCR showed that the protein expression level and mRNA transcript level of glutathione peroxidase 4 (GPX4) were significantly higher in the severe hypertrophy group (Figure 3F–H). The above results suggest that the ferroptosis process is significantly inhibited in tissues with severe adenoid hypertrophy.

Induction of Ferroptosis Reduce the Viability of Primary Adenoid Hypertrophy Cells

Since ferroptosis is closely associated with the severity of adenoid hypertrophy, we further investigated the effects of ferroptosis activation in primary adenoid cells. Cells were stimulated with LPS and conA (stimulation, STIM) to mimic hypertrophy and treated with the ferroptosis inducer RSL3 or the inhibitor Fer-1. The results showed that LPS+conA stimulation significantly promoted cell proliferation, whereas RSL3 treatment markedly inhibited this proliferation, and Fer-1 pretreatment partially restored the proliferative capacity (Figure 4A). GSH levels increased in the STIM group, decreased with RSL3, and were rescued by Fer-1 (Figure 4B). The trend of GPX4 protein expression was generally consistent with that of GSH, although the STIM group showed a slight increase compared with the control group without statistical significance (Figure 4C). RSL3 elevated ROS and Fe^{2+} levels, both attenuated by Fer-1 (Figure 4D and E). Taken together, these findings suggest that RSL3 can induce ferroptosis in primary adenoid cells and inhibit their proliferation. Subsequently, we examined the expression levels of hub genes, and the results showed that the transcript levels of *HSPA1B, HSPA1A, PLTP, HDLBP*, and *LDLR* were significantly reduced in the STIM+RSL3 group, while *HSPA13, HSPA14*, and were significantly increased. However, there was no significance difference in *PLA2G7* expression (Figure 4F and Table S5). These results confirm that the effect of ferroptosis in vitro.

Discussion

Adenoid hypertrophy is the major cause of OSA in children, yet its cellular and molecular mechanisms remain unclear. Our study is the first to identify key ferroptosis-related genes involved in adenoid hypertrophy, which were further validated in tissue samples by RT-qPCR. Tissue analyses revealed that marked downregulation of ferroptosis were increased with hypertrophy. Consistently, in a cellular model, RSL3-induced ferroptosis significantly suppressed cell proliferation, suggesting a potential role of ferroptosis in the progression of adenoid hypertrophy.

Previous studies have shown that in the liver of OSA patients, GPX4 and GSH levels are decreased, whereas iron and MDA levels are increased, suggesting that chronic intermittent hypoxia (CIH) promotes ferroptosis and contributes to the progression of nonalcoholic fatty liver disease.[14] Similarly, CIH model mice exhibit typical morphological changes of ferroptosis in the brain, accompanied by reduced neuronal survival.[15] In contrast, in hypertrophic adenoid tissues from children with OSA, we observed that ferroptosis decreased with increasing severity of adenoid hypertrophy. This may be explained by the fact that adenoid size cannot accurately reflect the severity of OSA, including either the total number of apnea events or the degree of hypoxia.[20,21] Second, the effect of hypoxia on ferroptosis varies by tissue and cell type. Hypoxia can upregulate hypoxia-inducible factor (HIF), which can either suppress ferroptosis directly or promote it through heme oxygenase-1 (HO-1) transcription.[22,23] In human tonsillar cells, hypoxia enhances HIF-1α activity via SUMO-1 upregulation.[24] Therefore, in adenoid cells, hypoxia may primarily activate HIF signaling and its downstream antioxidant programs, thereby reducing their susceptibility to ferroptosis. Finally, the local inflammatory milieu adds complexity. In children with adenoid hypertrophy, the levels of inflammatory factors such as TNF-α, IL-6, and IL-32 increase with the severity.[25] The crosstalk between inflammation and ferroptosis is not uniformly promotive and can yield divergent outcomes depending on the cellular context and cytokine profile.[26] Different degrees of adenoid hypertrophy may reflect distinct pathological states rather than a linear continuum. Variations in inflammatory cytokine profiles across these states could diverge in their effects on ferroptosis. Under CIH and sustained inflammation, adenoid cells may undergo adaptive changes, ultimately leading to reduced lipid peroxidation and iron levels, along with elevated GSH in severely hypertrophic adenoid tissue.

Emerging evidence indicates that ferroptosis may participate in several pediatric inflammatory conditions beyond adenoid hypertrophy. In asthma-related airway inflammation, allergen exposure and chronic inflammation can trigger ferritinophagy, creating a microenvironment that favors ferroptosis in bronchial epithelial cells, thereby promoting epithelial injury and airway hyperresponsiveness.[27] Similarly, in pediatric conditions such as chronic rhinosinusitis

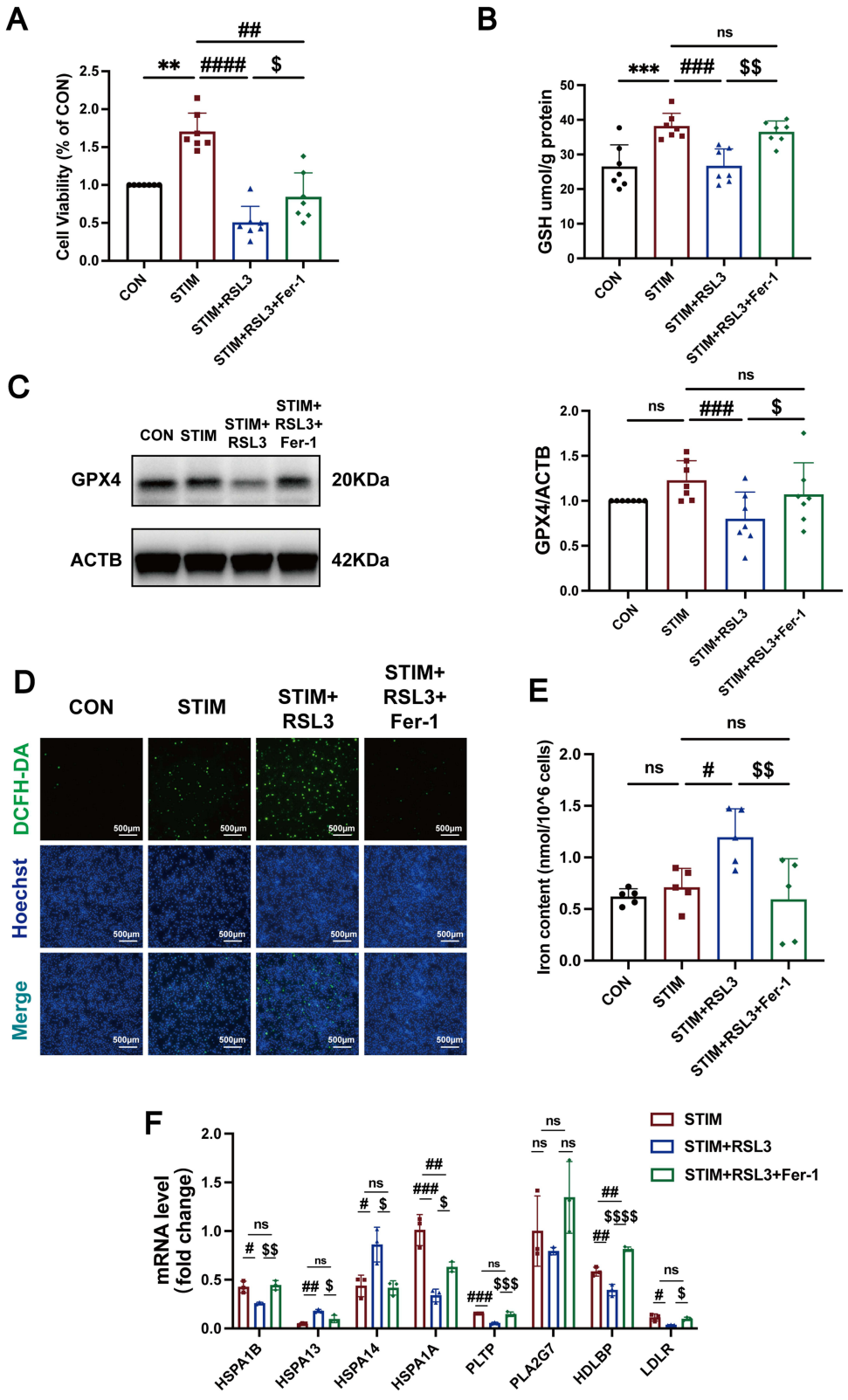

Figure 4 RSL3 induced ferroptosis suppresses the viability of primary adenoid cells and alters the transcription levels of ferroptosis hub genes. (**A**) CCK-8 assay for detecting the proliferation of primary adenoid cells. Data normalized to control group (set as 100%). n=7 per group. (**B**) Detection of the levels of GSH, n=7 per group. (**C**) Representative Western blot bands and average protein levels of GPX4, n=7 per group. (**D**) Intracellular ROS levels detected by DCFH-DA staining. (**E**) Ferrous ion content in cell, n=5 per group. (**F**) The mRNA expression of ferroptosis-related hub genes, data are normalized to the control group (set as 1, not shown in the figure), n=3 per group. Statistical significance was determined by one-way ANOVA. ns, not significant. Compared with the control group, $^{**}P < 0.01$, $^{***}P < 0.001$. Compared with the STIM group, $^{\#}P < 0.05$, $^{\#\#}P < 0.01$, $^{\#\#\#}P < 0.001$, $^{\#\#\#\#}P < 0.0001$. Compared with the STIM+RSL3 group, $^{\$}P < 0.05$, $^{\$\$}P < 0.01$, $^{\$\$\$}P < 0.001$, $^{\$\$\$\$}P < 0.0001$.

with nasal polyps,[28] Crohn's disease,[29] and pediatric sepsis,[30] ferroptosis in airway or intestinal epithelial cells disrupts barrier integrity and amplifies neutrophil-driven inflammation. In these contexts, ferroptosis is generally regarded as a pathogenic driver that exacerbates tissue injury and inflammatory responses. In contrast to this typically upregulated and detrimental process, our findings reveal a paradoxical decrease of ferroptosis in severely hypertrophic adenoids, suggesting a unique and potentially compensatory suppression of ferroptosis in the specific disease context of OSA-related adenoid hypertrophy.

We used the MCODE and CytoHubba plugins in Cytoscape to analyze the DEGs and identified 8 hub genes, which formed two functionally distinct clusters. The first cluster comprises 4 HSP70 family members (*HSPA1A, HSPA1B, HSPA13, HSPA14*), maintaining cellular homeostasis under environmental and physiological stress conditions.[31] In pediatric adenoid tissue, HSP70 is expressed and can modulate immune responses, suggesting a potential contribution to chronic inflammation and tissue remodeling.[32,33] Notably, *HSPA1A* and *HSPA1B* demonstrate specific immunomodulatory roles by regulating interferon signaling pathways, which directly impacts CD8+ T cell exhaustion and ferroptosis resistance.[34] Interestingly, previous studies have demonstrated that children with adenoid hypertrophy exhibit elevated interferon levels, and a reduction in CD8+ T cells in severe adenoid hypertrophy group.[35,36] A similar mechanism may underlie adenoid hypertrophy: chronic interferon activation leads to a reduction in CD8+ T cells, thereby establishing an immune microenvironment that favors cell survival while suppressing ferroptosis. While *HSPA13* and *HSPA14* maintain endoplasmic reticulum protein homeostasis and ribosome-associated protein folding respectively, their precise contributions to ferroptosis regulation in adenoid tissue warrant further investigation.[31] The second cluster encompasses lipid metabolism–related genes (*PLTP, PLA2G7, HDLBP, LDLR*) that collectively modulate cellular ferroptosis susceptibility through lipid homeostasis. *PLTP* and *PLA2G7* primarily participate in lipid transport and oxidized phospholipid clearance, while *HDLBP* and *LDLR* regulate cholesterol balance, thereby suppressing ferroptosis.[37–39] Although the specific roles of these genes in adenoid hypertrophy remain unclear, children with adenoid hypertrophy commonly exhibit lipid metabolism disorders, characterized by decreased HDL-C and elevated LDL-C levels.[40,41] Therefore, we speculate that lipid metabolism disorders may alter the ferroptosis threshold of cells through this cluster of hub genes, contributing to disease progression. These pathways may also offer therapeutic potential. Modulators of ferroptosis, such as inducers or inhibitors, have demonstrated efficacy in preclinical models of inflammatory and hyperplastic disorders,[42] suggesting that targeting the HSP70-mediated stress response or the lipid metabolism–ferroptosis axis could be explored as potential strategies for adenoid hypertrophy in future studies.

To our knowledge, this is the first study to identify key ferroptosis-related genes associated with adenoid hypertrophy and assess their functional role in both tissue and cellular models. Our findings reveal an additional and previously unrecognized pathophysiologic pathway. Critically, we demonstrate that suppressed ferroptosis is associated with increased adenoid hypertrophy. In contrast to the prevailing view that ferroptosis contributes to tissue injury, our results highlight its protective role in this specific pathology. Thus, we identify ferroptosis-related alterations as a novel component of the disease process, providing new biological insights into adenoid hypertrophy. The consistent expression patterns of several ferroptosis-related hub genes across both RNA-seq and qRT-PCR validation suggest their potential as molecular indicators of adenoid hypertrophy severity and offer promising therapeutic targets beyond traditional inflammation-based approaches. Nevertheless, our study has several limitations. First, we demonstrated only an association between ferroptosis and the progression of adenoid hypertrophy; the causal relationship and the extent of ferroptosis' contribution remain to be further elucidated. Second, due to ethical constraints, we were unable to obtain adenoid tissues from healthy children and had to use mildly to moderately hypertrophic adenoids as controls. The findings reflect changes across the progression of hypertrophy rather than differences from a truly healthy baseline. This constitutes a potential source of bias and may limit the generalizability of the findings, which should be interpreted within this context. Third, the sample size for transcriptome sequencing was limited, which may affect the representativeness of the data. Fourth, although primary adenoid cells partially mimicked the in vivo environment, the complex cellular composition of adenoids prevented detailed exploration of the metabolic mechanisms linking ferroptosis to disease progression. Lastly, the absence of in vivo experiments limits causal inference. Future studies incorporating animal models or prospective clinical follow-up will be needed to further prove causation and confirm the mechanistic involvement of ferroptosis in adenoid hypertrophy.

Conclusion

In conclusion, our study identified certain ferroptosis-related genes associated with adenoid hypertrophy through bioinformatics analysis and in vitro studies. These findings suggest that impaired ferroptosis may promote tissue hypertrophy by enhancing cellular survival and resistance to oxidative stress. Targeting ferroptosis pathways may help develop novel anti-hypertrophic or anti-inflammatory strategies for children with OSA, potentially alleviating pediatric airway obstruction. Furthermore, ferroptosis-related markers may serve as promising biomarkers for assessing disease severity or treatment response. Future in vivo studies and validation in larger cohorts are warranted to confirm these mechanisms and advance translational applications.

Abbreviations

OSA, Obstructive Sleep Apnea; DEGs, differentially expressed genes; PPI, protein-protein interaction; KEGG, Kyoto Encyclopedia of Genes and Genomes; GSH, glutathione; ROS, reactive oxygen species; GO, Gene ontology; MF, molecular function; CC, cellular component; BP, biological process; LPS, lipopolysaccharide; conA, concanavalin A; Fer-1, Ferrostatin-1; MDA, malondialdehyde; GPX4, glutathione peroxidase 4; CIH, chronic intermittent hypoxia; HIF, hypoxia-inducible factor.

Data Sharing Statement

The original data provided in this study can be obtained from the corresponding author upon reasonable request.

Ethics Statement

This study was conducted in accordance with the Declaration of Helsinki and was approved by the Ethics Committee of Shanghai Children's Hospital (approval No.2025RY075-E01), and informed consent was obtained from the legal guardians.

Acknowledgments

We sincerely thank all the participants and their families for their valuable contributions and support to this study.

Author Contributions

All authors made substantial contributions to the reported work, including conceptualization, study design, execution, acquisition of data, analysis and interpretation. Using the CRediT taxonomy, the specific contributions are as follows:

Zilu Shen: Conceptualization, Investigation, Methodology, Resources, Software, Validation, Visualization, Writing-original draft, Writing-review & editing. Jingning Huang: Data curation, Formal analysis, Visualization, Writing-original draft, Writing-review & editing. Yunqiu Chu: Conceptualization, Formal analysis, Methodology, Supervision, Validation, Writing-original draft. Xiaoman Zhang: Conceptualization, Data curation, Project administration, Writing-review & editing. Huajun Xu: Conceptualization, Methodology, Project administration, Writing-review & editing. Hongming Xu: Formal analysis, Methodology, Supervision, Writing-review & editing. Jian Guan: Investigation, Resources, Software, Validation, Writing-review & editing. Meizhen Gu: Conceptualization, Funding acquisition, Project administration, Resources, Supervision, Writing-review & editing.

All authors have read and approved the final version of the paper, have agreed on the journal to which this paper was submitted, and accept responsibility for all aspects of the work.

Funding

This work was supported by grants from the National Natural Science Foundation of China (No. 82071029).

Disclosure

The authors declare that they have no competing interests.

References

1. Lévy P, Kohler M, McNicholas WT, et al. Obstructive sleep apnoea syndrome. *Nat Rev Dis Primers*. 2015;1:15015. doi:10.1038/nrdp.2015.15
2. Marcus CL, Brooks LJ, Draper KA, et al. Diagnosis and management of childhood obstructive sleep apnea syndrome. *Pediatrics*. 2012;130(3):e714–55. doi:10.1542/peds.2012-1672
3. Niedzielski A, Chmielik LP, Mielnik-Niedzielska G, Kasprzyk A, Bogusławska J. Adenoid hypertrophy in children: a narrative review of pathogenesis and clinical relevance. *BMJ Paediatr Open*. 2023;7(1). doi:10.1136/bmjpo-2022-001710
4. Guilleminault C, Korobkin R, Winkle R. A review of 50 children with obstructive sleep apnea syndrome. *Lung*. 1981;159(5):275–287. doi:10.1007/bf02713925
5. Zhang J, Sun X, Zhong L, Shen B. IL-32 exacerbates adenoid hypertrophy via activating NLRP3-mediated cell pyroptosis, which promotes inflammation. *Mol Med Rep*. 2021;23(3). doi:10.3892/mmr.2021.11865
6. Yilmaz T, Koçan EG, Besler HT. The role of oxidants and antioxidants in chronic tonsillitis and adenoid hypertrophy in children. *Int J Pediatr Otorhinolaryngol*. 2004;68(8):1053–1058. doi:10.1016/j.ijporl.2004.04.003
7. Dixon SJ, Lemberg KM, Lamprecht MR, et al. Ferroptosis: an iron-dependent form of nonapoptotic cell death. *Cell*. 2012;149(5):1060–1072. doi:10.1016/j.cell.2012.03.042
8. Fang X, Wang H, Han D, et al. Ferroptosis as a target for protection against cardiomyopathy. *Proc Natl Acad Sci U S A*. 2019;116(7):2672–2680. doi:10.1073/pnas.1821022116
9. Li Q, Han X, Lan X, et al. Inhibition of neuronal ferroptosis protects hemorrhagic brain. *JCI Insight*. 2017;2(7):e90777. doi:10.1172/jci.insight.90777
10. Liu P, Zhao D, Pan Z, Tang W, Chen H, Hu K. Identification and validation of ferroptosis-related hub genes in obstructive sleep apnea syndrome. *Front Neurol*. 2023;14:1130378. doi:10.3389/fneur.2023.1130378
11. Huang J, Zhang H, Cao L, et al. Ferroptosis-related genes are considered as potential targets for CPAP treatment of obstructive sleep apnea. *Front Neurol*. 2023;14:1320954. doi:10.3389/fneur.2023.1320954
12. Xu W, Chi L, Row BW, et al. Increased oxidative stress is associated with chronic intermittent hypoxia-mediated brain cortical neuronal cell apoptosis in a mouse model of sleep apnea. *Neuroscience*. 2004;126(2):313–323. doi:10.1016/j.neuroscience.2004.03.055
13. Seifen C, Pordzik J, Huppertz T, et al. Serum Ferritin Levels in Severe Obstructive Sleep Apnea. *Diagnostics*. 2023;13(6). doi:10.3390/diagnostics13061154
14. Cai W, Wu S, Ming X, et al. IL6 derived from macrophages under intermittent hypoxia exacerbates NAFLD by promoting ferroptosis via MARCH3-Led ubiquitylation of GPX4. *Adv Sci*. 2024;11(41):e2402241. doi:10.1002/advs.202402241
15. Zhong P, Li L, Feng X, et al. Neuronal ferroptosis and ferroptosis-mediated endoplasmic reticulum stress: implications in cognitive dysfunction induced by chronic intermittent hypoxia in mice. *Int Immunopharmacol*. 2024;138:112579. doi:10.1016/j.intimp.2024.112579
16. Gharib SA, Hayes AL, Rosen MJ, Patel SR. A pathway-based analysis on the effects of obstructive sleep apnea in modulating visceral fat transcriptome. *Sleep*. 2013;36(1):23–30. doi:10.5665/sleep.2294
17. Kheirandish-Gozal L, Serpero LD, Dayyat E, et al. Corticosteroids suppress in vitro tonsillar proliferation in children with obstructive sleep apnoea. *Eur Respir J*. 2009;33(5):1077–1084. doi:10.1183/09031936.00130608
18. Xu Y, Li Y, Li J, Chen W. Ethyl carbamate triggers ferroptosis in liver through inhibiting GSH synthesis and suppressing Nrf2 activation. *Redox Biol*. 2022;53:102349. doi:10.1016/j.redox.2022.102349
19. Jiang L, Kon N, Li T, et al. Ferroptosis as a p53-mediated activity during tumour suppression. *Nature*. 2015;520(7545):57–62. doi:10.1038/nature14344
20. Brooks LJ, Stephens BM, Bacevice AM. Adenoid size is related to severity but not the number of episodes of obstructive apnea in children. *J Pediatr*. 1998;132(4):682–686. doi:10.1016/s0022-3476(98)70360-9
21. Cai J, Xiu T, Song Y, et al. Deep learning-based quantification of adenoid hypertrophy and its correlation with apnea-hypopnea index in pediatric obstructive sleep apnea. *Nat Sci Sleep*. 2024;16:2243–2256. doi:10.2147/nss.S492146
22. Feng X, Wang S, Sun Z, et al. Ferroptosis enhanced diabetic renal tubular injury via HIF-1α/HO-1 Pathway in db/db mice. *Front Endocrinol*. 2021;12:626390. doi:10.3389/fendo.2021.626390
23. Xiong J, Nie M, Fu C, et al. Hypoxia enhances HIF1α transcription activity by upregulating KDM4A and mediating H3K9me3, thus inducing ferroptosis resistance in cervical cancer cells. *Stem Cells Int*. 2022;2022:1608806. doi:10.1155/2022/1608806
24. Lin Y, Wang M, Xiao Z, Jiang Z. Hypoxia activates SUMO-1-HIF-1α signaling pathway to upregulate pro-inflammatory cytokines and permeability in human tonsil epithelial cells. *Life Sci*. 2021;276:119432. doi:10.1016/j.lfs.2021.119432
25. Wang H, Bai J, Zhang J, Yang W, Zuo K, Li H. IL-6 promotes the expression of vascular endothelial growth factor through the p38 signalling pathway in hypertrophied adenoids in children. *Int J Pediatr Otorhinolaryngol*. 2013;77(2):205–209. doi:10.1016/j.ijporl.2012.09.040
26. Chen Y, Fang ZM, Yi X, Wei X, Jiang DS. The interaction between ferroptosis and inflammatory signaling pathways. *Cell Death Dis*. 2023;14(3):205. doi:10.1038/s41419-023-05716-0
27. Zeng Z, Huang H, Zhang J, et al. HDM induce airway epithelial cell ferroptosis and promote inflammation by activating ferritinophagy in asthma. *FASEB J*. 2022;36(6):e22359. doi:10.1096/fj.202101977RR
28. Pan L, Yu Z, Xiang WX, et al. Cigarette smoke-induced epithelial cell ferroptosis promotes neutrophilic inflammation in patients with nasal polyps. *J Allergy Clin Immunol*. 2025;155(6):1882–1897. doi:10.1016/j.jaci.2025.02.034
29. Lin P, Xu S, Yan X, Zhuang X. Identification of ferroptosis-related genes in pediatric Crohn's disease using bioinformatics approaches. *Sci Rep*. 2025;15(1):37830. doi:10.1038/s41598-025-21703-1
30. Li Z, Zhang C, Liu Y, et al. Diagnostic and predictive values of ferroptosis-related genes in child sepsis. *Front Immunol*. 2022;13:881914. doi:10.3389/fimmu.2022.881914
31. Rosenzweig R, Nillegoda NB, Mayer MP, Bukau B. The Hsp70 chaperone network. *Nat Rev Mol Cell Biol*. 2019;20(11):665–680. doi:10.1038/s41580-019-0133-3
32. Min HJ, Park JS, Kim CE, Kim KS. Profiling of heat shock proteins 27 and 70 in adenoids of children. *Eur Arch Otorhinolaryngol*. 2019;276(9):2483–2489. doi:10.1007/s00405-019-05528-z

33. Aktepe F, Sahin O, Dilek H, Yilmaz D, Kahveci O, Derekoy S. Immunohistochemical assesment of heat shock protein 70 in adenoid tissue. *Int J Pediatr Otorhinolaryngol*. 2007;71(6):857–861. doi:10.1016/j.ijporl.2007.02.017
34. Hu W, Zhao Z, Du J, et al. Interferon signaling and ferroptosis in tumor immunology and therapy. *NPJ Precis Oncol*. 2024;8(1):177. doi:10.1038/s41698-024-00668-w
35. Zhu Y, Wang S, Yang Y, et al. Adenoid lymphocyte heterogeneity in pediatric adenoid hypertrophy and obstructive sleep apnea. *Front Immunol*. 2023;14:1186258. doi:10.3389/fimmu.2023.1186258
36. Marcano-Acuña ME, Carrasco-Llatas M, Tortajada-Girbés M, Dalmau-Galofre J, Codoñer-Franch P. Impact of adenotonsillectomy on the evolution of inflammatory markers. *Clin Otolaryngol*. 2019;44(6):983–988. doi:10.1111/coa.13423
37. Goldstein I, Ezra O, Rivlin N, et al. p53, a novel regulator of lipid metabolism pathways. *J Hepatol*. 2012;56(3):656–662. doi:10.1016/j.jhep.2011.08.022
38. Vermonden P, Martin M, Glowacka K, et al. Phospholipase PLA2G7 is complementary to GPX4 in mitigating punicic-acid-induced ferroptosis in prostate cancer cells. *iScience*. 2024;27(5):109774. doi:10.1016/j.isci.2024.109774
39. Xian M, Wang Q, Xiao L, et al. Leukocyte immunoglobulin-like receptor B1 (LILRB1) protects human multiple myeloma cells from ferroptosis by maintaining cholesterol homeostasis. *Nat Commun*. 2024;15(1):5767. doi:10.1038/s41467-024-50073-x
40. Zong J, Liu Y, Huang Y, et al. Serum lipids alterations in adenoid hypertrophy or adenotonsillar hypertrophy children with sleep disordered breathing. *Int J Pediatr Otorhinolaryngol*. 2013;77(5):717–720. doi:10.1016/j.ijporl.2013.01.025
41. Gozal D, Capdevila OS, Kheirandish-Gozal L. Metabolic alterations and systemic inflammation in obstructive sleep apnea among nonobese and obese prepubertal children. *Am J Respir Crit Care Med*. 2008;177(10):1142–1149. doi:10.1164/rccm.200711-1670OC
42. Tao L, Yang X, Ge C, et al. Integrative clinical and preclinical studies identify FerroTerminator1 as a potent therapeutic drug for MASH. *Cell Metab*. 2024;36(10):2190–2206.e5. doi:10.1016/j.cmet.2024.07.013